CHAPTER 5

COUNTERFLOW FACILITIES

by

Robert J. Carros and Charles E. DeRose

NASA-Ames Research Center

COUNTERFLOW FACILITIES

Robert J. Carros and Charles E. DeRose

5.1 INTRODUCTION

In ballistic testing, the maximum velocity is limited by structural limitations of the model and sabot and by the velocity capabilities of the gun. Though these limits have been steadily pushed higher through changes in gun operating cycles and design, availability of stronger materials for model and sabot construction, and advanced construction techniques, the interest in very high-speed phenomena motivated by space vehicles and basic research problems seem always to demand a velocity higher than that available. To satisfy this demand, for aerodynamic studies, a test section with a high-speed airstream may be combined with a conventional ballistic range to produce what has been called a counterflow facility. With this combination facility, the airstream velocity is added directly to the model velocity.

Typically, the counterflow facility consists of a long test section (by usual wind-tunnel standards) in which a supersonic airstream of near-constant stream properties is established. The model is launched upstream through this test section so that the total velocity experienced is equal to the sum of the model launch velocity and the airstream velocity. Data are recorded photographically as in conventional ballistic facilities, the only additional factor being that of accurately determining the airstream properties – pressure, temperature, and velocity.

The major advantage of the counterflow facility is that of increasing the velocity capability for aerodynamic testing with a given gun-model combination. However, it is not the only benefit realized. By control of the free-stream temperature, the Mach number can be varied considerably. Extremely high Mach numbers can be obtained by using a cold stream. Free-stream temperatures in the order of 100° K are easy to obtain and, with the speed of sound at this temperature around 200 meters/second, it is seen that a reasonable model velocity of 6 km/sec can yield Mach numbers of the order of 30 or more. In the same vein, a change in the free-stream temperature brings about a change in Reynolds number capability. Hot airstreams generated with high-energy drive systems produce low Reynolds numbers, while, conversely, cold airstreams will be characterized by high Reynolds numbers.

Another benefit is that the total model flightpath can be lengthened by the use of a high airstream velocity coupled with a low model velocity. Since the model flightpath length relative to the airstream is equal to

$$L_T = L_{ts} + V_t\left(\frac{L_{ts}}{V_m}\right) \tag{5.1}$$

$$L_T = L_{ts}\left(1 + \frac{V_t}{V_m}\right), \tag{5.2}$$

where V_m = velocity of model alone, m/sec

V_t = velocity of tunnel airstream, m/sec

L_{ts} = length of test section, m

L_T = total resultant flightpath length, m

it can be seen that the total flightpath length can easily be stretched out far beyond the actual test-section length. This capability contributes generally to the accuracy of aerodynamic measurements which improve with increasing range length, and in particular can be important when conducting tests to determine static and dynamic stability of a model where flightpath lengths must be of the order of two or more wave-lengths of pitch oscillation.

The counterflow type of facility also affords the capability – with suitably designed nozzles and test section – of permitting model flights through a variable density profile. Simulation of an earth entry for a space probe can be accomplished by a facility of this type. This kind of facility is highly restricted in the breadth of its research, but it is unique in offering a predetermined density, temperature, and velocity variation along the model flightpath.

Finally, another variation of a counterflow facility can be used to study the effect of blast waves on models in free flight. The use of a free-flying model allows the opportunity to observe the results of both a shock wave's dynamic effect on the model, and its aerodynamic effect on the bow shock wave, boundary layer, and wake, etc. The facility for this kind of study is essentially a launch gun firing a model into a shock tube.

All of the aforementioned capabilities are extensions of the basic capability of a conventional ballistic facility. At the same time, the use of a counterflow airstream complicates the testing and increases the cost of building and operating the facility. However, the difficulties can be largely overcome, and the benefits that this type of facility can offer in the form of greatly increased testing range are, for certain applications, well worth the effort.

To illustrate the operating parameters and some of the inherent problems involved with operating a counterflow facility, we will examine the two major varieties in use. The first type will be designated the continuous flow facility – typified by the blow-down, unheated reservoir, wind tunnel. By continuous flow, we mean that the airflow duration is very long compared to the time of flight of the model. Flow times may be of the order of a minute or two which permits manual control of the test section conditions and the gun-firing sequence. The second type will be called the short-duration facility, in which the airflow times are only slightly longer than the flight time of the model. Typical of this latter type is the shock-tube-driven wind-tunnel configuration. Here, timing is of the utmost importance and most events in the launch procedure must be preprogrammed and sequenced by electronic control.

5.2 LONG-DURATION COUNTERFLOW BALLISTIC FACILITIES

5.2.1 General Description

Perhaps the simplest form of counterflow ballistic facility is one that utilizes a supersonic blow-down wind tunnel. The supersonic tunnel used in this way differs from a conventional blow-down tunnel mainly in the longer test section and the greater number of observation stations. Lengthening of the test section requires a divergence to the tunnel walls to account for boundary-layer growth. A maximum airstream velocity of approximately 0.6 km/sec can be attained without heating the supply air. This stream velocity of 0.6 km/sec for a Mach number 3 airflow, for example, when combined with a model velocity of 3 km/sec, results in a test Mach number of 18. (When an unheated air supply is expanded to a Mach number 3 airstream, the resultant sound speed is approximately 0.2 km/sec). The airstream density is relatively high (for this Mach number, 0.076 times the density in the air reservoir). The minimum density depends on the diffuser and exhaust conditions of the wind tunnel. For example, specification of atmospheric exhaust pressure with a blow-down wind tunnel determines the minimum reservoir pressure at which the tunnel will operate.

The complications to the testing introduced by combining a ballistic range and supersonic blow-down tunnel are not great. The first consideration is of course that of introducing the test model into the airstream at the proper time. This, fortunately, can be done quite easily, requiring no electronic sequence timers, since the time-of-model flight through the test section is very short, only a few milliseconds, compared to the long airflow duration of the order of a minute. The test operator can very easily fire the gun at a time when airflow has been properly established in the test section. Details of operation and instrumentation of a ballistic range will be found in other sections of this book and details of wind-tunnel operation and instrumentation can be found in the literature (see, for example, Reference 5.1), and will not be discussed here.

5.2.2 The Ames Supersonic Free-Flight Wind Tunnel

The facility described in this section was proposed by H.Julian Allen in 1946 as a means of extending the range of Mach numbers for laboratory aerodynamic testing beyond what was then available in wind tunnels. The Supersonic Free-Flight Wind Tunnel, placed in operation at the Ames Laboratory of National Advisory Committee for Aeronautics (NACA) in 1949, is shown schematically in Figure 5.1 and was the first counterflow ballistic facility. A brief description of the facility will be given here and a more complete description is contained in Reference 5.2.

5.2.2.1 Description of Facility

Air from an unheated reservoir, available to a maximum pressure of 6 atm, was expanded to Mach number 2 through a two-dimensional nozzle and exhausted to atmosphere. The most striking differences between this tunnel and a conventional supersonic blow-down tunnel was the test section length and the number of windowed observation stations. The test section originally was approximately 4.6 meters long and contained four vertical and three horizontal observation stations. After an initial operating period of five years demonstrated that the facility was both technically feasible and valuable, the test section was modified in 1955 to increase its length to approximately 7.3 meters with nine orthogonal photographic stations spaced at intervals of 0.915 meters. An additional interchangeable nozzle was added at this time for Mach number 3 airflow. The test section width originally was approximately 30 centimeters and height was approximately 61 centimeters, while the modified test section was approximately 43 cm wide by nominally 51 cm high. A photograph of the test section is shown in Figure 5.2.

The unusual length of the test section does not introduce any fundamental difficulties. It has been found that such a long supersonic flow can be established and maintained, with no more unsteadiness than is usual to supersonic wind-tunnel flows. Interestingly enough, it is found that when the reservoir pressure is reduced to the minimum levels that will sustain supersonic flow, the downstream end of the test section may lose supersonic flow while the upstream end retains it. However, the most important problem associated with the long test section is the growth of the thick turbulent boundary layer on the walls. This boundary layer would, in a long enough test section, ultimately fill the channel and leave no core of turbulence-free air for testing. The Supersonic Free-Flight Wind Tunnel and the subsequent Ames counterflow facilities were designed so that

this would not occur within the test section, and this specification in effect determined the minimum width dimensions of the facilities.

The time-average boundary-layer thicknesses in the Supersonic Free-Flight Wind Tunnel were calculated to be between 10 and 13 cm depending on stream Mach number and Reynolds number. With the final test section dimensions, this left a turbulence-free core at least 18 cm wide by about 36 cm high at the downstream end of the test section (station 1). This width was easily adequate for testing, since the model dispersion is least at this end of this test section, which is the end nearest the launching gun.

The displacement effect of the boundary layer also had to be considered, since for a uniform test-section cross section it would effectively diminish the area available for supersonic flow and thus reduce the Mach number with distance from the nozzle. To avoid this source of stream nonuniformity, the upper and lower blocks of the test section were designed to diverge and to compensate on two walls for the boundary-layer displacement thickness on four walls. Displacement thicknesses were calculated to be of the order of 2.5 cm at the downstream end of the test section, and the divergence allowed on the upper and lower blocks was slightly greater than 5 cm on each, giving a downstream end height of the channel of about 61 cm actual as compared to 51 cm nominal. As the stream Mach number and reservoir pressure were varied, this setting was not perfect, but represented a compromise or best average position, which was weighted in favor of the test condition most often used – the Mach number 3 airflow near maximum reservoir pressure. Some axial pressure variation thus remained for some flow conditions, and this will be described in a later section. It was not deemed practical or necessary to make the test section adjustable to best fit the airflow condition being used on each run.

The diffuser section had two right angle bends to greatly reduce the amount of daylight reaching the photographic film to prevent fogging. Furthermore, all surfaces in the diffuser and test section were painted with flat black paint to reduce the light reflecting back to the test section and the shadowgraph film. Curved vanes were located at the first bend in the diffuser to turn the air smoothly.

The model-launching gun was mounted on an "I" beam anchored to the floor of the diffuser. The beam and gun mounts were arranged so that the centerline of the gun was coincident with the axis of the tunnel test section. A model catcher located in the settling chamber was filled with fireproof cotton waste backed up by several thick steel plates.

As in a conventional blowdown tunnel, pressure and temperature were measured from which the necessary stream properties were obtained. The instrumentation used to record data pertaining to the model was identical to that used in a ballistic range and is described in detail in other sections of this book.

5.2.2.2 Range of Test Conditions

The range of test conditions that were available in the Supersonic Free-Flight Wind Tunnel are shown in Figures 5.3 and 5.4. The test Mach number range is given for model-launching velocities to 6 km/sec. This velocity is well within the capability of modern light-gas guns which have operated to a maximum speed of 11.3 km/sec at Ames Research Center in 1966. The original Supersonic Free-Flight Wind Tunnel, however, never operated beyond a model-launching velocity of 3.7 km/sec corresponding to a maximum test Mach number of 21. There were three reasons for this limitation. First, the peak utilization of the original facility occurred before the present high level of gun capability was developed. Second, the gun beam provided in the facility was not long enough to accommodate the greater lengths of any but small-caliber light-gas guns. Third, the self-luminosity of the flow fields at very high speeds tends to fog the shadowgraph pictures and obliterate the model image (see for example, Figure 6.33 in Chapter 6). All of these problems could have been overcome, and, in fact, steps were required and were taken to modify the shadowgraph stations to overcome the third problem even at velocities of 3.7 km/sec; but at the same time, the higher performance, short-duration counterflow facilities were being developed, so emphasis was placed on them and use of the Supersonic Free-Flight Wind Tunnel was phased out.

The Mach number for a test utilizing the airstream is the sum of the stream Mach number and the model Mach number. (The sound speed is 0.253 km/sec for an air reservoir at room temperature with the Mach 2 airstream, and 0.204 km/sec with the Mach number 3 airstream). A test program using the facility air-off and air-on can, in principle, easily cover a range of supersonic Mach numbers up to 33.

The Reynolds number capability is shown in Figure 5.4 and extends over a wide range to a maximum of approximately 10 million per centimeter. Early in 1959 the Supersonic Free-Flight Wind Tunnel was connected to a 9½-atm air-supply reservoir. This increased the maximum Reynolds numbers available by a factor of 1.5.

5.2.2.3 Effect of Airstream Variations on Tests

The airstreams in supersonic wind tunnels are invariably imperfect and surveys of the airflow in the long test section of the Ames Supersonic Free-Flight Wind Tunnel disclosed a number of departures from uniform flow. A brief description of these and their effect on the aerodynamic data obtained from the facility will now be discussed.

The observed longitudinal variation of Mach Number, shown in Figure 5.5, was small, being only approximately ± ½% at M = 2 and ± ¼% at M = 3. The growth of the boundary layer, as discussed in Section 5.2.2.1, is responsible for the observed decrease in Mach number at the downstream (station 1) end of the test section for the

M = 3 condition and demonstrates that the cross-sectional area of the test section was insufficient to accommodate the thickened boundary layer. On the other hand, the small variation observed in the Mach number at the M = 2 condition shows that, in this case, the test-section area was adequate to allow for the boundary-layer growth. Early during calibration some adjustments were made to the cross-sectional area, by increasing the height dimension, to select the best setting that would result in the most favorable Mach number distribution for both the M = 2 and M = 3 conditions. Since the total test Mach number was high (for example, for a rather modest model velocity of 1.5 km/sec the total Mach number is approximately 10.5 for the M = 3 airstream) the small Mach number variation observed was not sufficient to effect aerodynamic data.

Closely associated with the Mach number variation are variations in the static and dynamic pressures. These are shown in Figure 5.6. The static-pressure-gradient results in buoyancy forces which are small compared to the drag forces and therefore do not affect the data significantly. The dynamic pressure varied approximately 0.7% at M = 2 and 1½% at M = 3 and this variation did cause some scatter in the results.

The variation of Mach number, static pressure, and dynamic pressure across the stream at station 1 is shown in Figure 5.7 for M = 2 and Figure 5.8 for M = 3 . The variation in the central 5-centimeter core of the flow, where most model flights take place at this station nearest the gun, was small. From shadowgraph photographs showing the boundary layer and from oscillations observed in the manometer used to read total head pressures, as shown in Figure 5.9, it was evident that the boundary layer was approaching to within 5-centimeters of the tunnel centerline and was undoubtedly the cause for the variations observed in Figures 5.7 and 5.8.

Measurements of airstream angularity were attempted using cones that were pivoted so that they could become aligned with the stream. Photographs of the cones, made with a high-speed motion-picture camera, showed that they oscillated with an amplitude of about ±2 degrees at frequencies matching the natural frequency of the cones. Since the frequency of variation of the stream angle was several times that of the natural frequency in pitch of the test models, the pitching response of the test models to the stream angle variation was weak. Furthermore, the effect of stream angularity on a moving model is less than on a stationary model, as shown by the ratio

$$\frac{u_a}{V_a + V_m}, \tag{5.3}$$

where u_a = lateral velocity component of airstream

V_a = airstream velocity relative to earth

V_m = model velocity relative to earth

which defines stream angle relative to a moving model. For example, a model flying at a Mach number of 3 in the Mach number 3 airstream (total test Mach number of 6) would experience only one-half the stream angle that a stationary model would experience. It was concluded that the influence of the observed stream-angle variation and the variations observed in Mach number, static and dynamic pressures were small and resulted in no important errors.

5.2.3 Atmosphere-Entry Simulators

5.2.3.1 Description of Facility

A second and rather specialized counterflow facility to simulate the velocity history and heating of entry vehicles coming into the earth's atmosphere has been mentioned in the Introduction. This type of facility makes use of a long contoured nozzle to dynamically establish a density profile along the nozzle axis which presents to the free-flight model flying upstream a variation similar to that encountered by a vehicle entering the atmosphere. The degree of simulation of entry aerodynamic heating which results has been shown to be surprisingly complete [5.3].

Such a facility was built at Ames Research Center and placed in operation in 1960. It consists of a high-pressure air reservoir, the specially contoured test-section nozzle, a vacuum tank, and a light-gas model-launching gun. Figure 5.10 is a schematic diagram of this facility and Figure 5.11 is a photograph of the air reservoir, test section, and large diameter piping leading to the vacuum sphere. The expanding test section was approximately 12 meters long, and during airflow, the air density varied exponentially with distance to simulate the variation with altitude in the atmosphere. Approximately three decades of density variation occurred within the test section so that an altitude interval of about 45 km in the earth's atmosphere was simulated. The actual air densities were larger than atmospheric by the scale factor of the model tested in order to achieve Reynolds number and heating simulation [5.3].

Airflow was supplied by a 0.48-cubic-meter high-pressure vessel initially pressurized up to 45 atm with air at room temperature. Mechanically rupturing the diaphragm between the reservoir and test section initiated flow which was exhausted into a 9¾ meters diameter vacuum sphere. The test section was instrumented with 12 orthogonal pairs of shadowgraph stations, as well as with static pressure transducers located at the sidewall to define the actual variation of air density with distance.

The model-launching gun used with this facility was a two-stage, light-weight piston (shock-heated) light-gas gun, with launch tube diamters of 12.7 and 20mm. The gun is required to launch the model at the velocity at which the vehicle to be simulated enters the atmosphere. A more detailed description of this facility will be found in Reference 5.4.

5.3 SHORT-DURATION, HIGH-ENERGY AIR SUPPLY SYSTEMS

The facilities in Section 5.2 all operate with room temperature air supplies and, as a result, are limited to airstream velocities of about 0.6 km/sec. When very high test speeds are desired, in the range from 10 to 15 km/sec, it would seem desirable to attempt to realize a larger speed increment from the airstream. In order to do so, it is necessary to utilize high-energy, heated reservoir types of drive systems. As the airstream velocity is increased, the required temperature of the reservoir quickly exceeds the limits of standard construction materials. Figure 5.12 shows the reservoir temperature required to produce a given stream velocity. The assumption is made that the airstream produced has a constant Mach number 7. The only way to obtain the high airstream velocities desired (from 2 km/sec and above) is to operate the facility in a manner in which the reservoir air is held for an extremely short time. As ballistic tests normally have flight times in the millisecond range, the use of a high-energy, short-duration-type of facility seems particularly attractive.

Although a number of possible approaches to a short-duration, high-energy supply are conceivable, at this writing there exists experience with only one – the reflected-shock (tailored-interface) shock tube [5.5-5.13]. Other possibilities which have not been developed would include arc-heated air supplies (hot-shot wind-tunnel type), piston compression reservoir heaters[5.14-5.18], and electrical resistance heated air supplies. The latter two types were seriously reviewed at Ames Research Centre prior to the construction of the facilities described later, and were judged to have considerable problems. Still another possibility that was considered to the extent that development tests were carried out was the use of gun-powder gases as a shock-tube driver system. Thus, although the remaining discussion is restricted to combustion-heated and cold helium shock-tube drivers, the basic concept need not be restricted in the reader's mind to this approach.

5.3.1 Shock-Tube Wind-Tunnel Configurations

The one type of system which has been applied to high-performance counterflow ballistic testing uses a shock-tube driver to supply air for a wind-tunnel test section, as in Figure 5.13. As shown in the figure, the shock-tube driven, counterflow ballistic range is composed of six component parts.

The first two, the driver and shock-tube, create the reservoir of high-temperature test gas. The driver section is filled with high-pressure gases such as hydrogen or helium, and the shock-tube, with low-pressure air (or other test gas). The two sections are separated by the main diaphragm, the explosively-triggered rupture of which starts the gas-compression cycle. The driver performance may be enhanced by heating the driver gas just prior to bursting the main diaphragm, either by chemical reactions in the driver (e.g., burning hydrogen), electrical heating, or compression heating. Basic theory and operation of shock tubes can be found in numerous reports, examples of which are References 5.5 to 5.13. The emphasis here will be on special aspects relating to their use as a counterflow air-supply system.

These first two tubes represent the high-pressure section of the facility and must be constructed to hold and seal against an internal pressure measuring as high as 1000 to 2000 atm. This high pressure is required for reasonable airstream densities in the test section if airstream velocities above 3 km/sec are contemplated.

Beyond the shock-tube, the end of which is the high-energy reservoir, are the nozzle section, test section and receiver tank, the low-pressure section of the facility. Here the pressure has to be reduced initially to the order of 100 microns of mercury (0.00013 atm) to permit the airflow to be established. This level of vacuum requires very careful attention to seals, piping, and valves, and a good quality mechanical vacuum pumping installation. As noted in Figure 5.13, the volume of the receiver tank is preferably designed to contain all of the gas without raising the resultant pressure above the safety limit of the glass windows in the test section. Frequently, in the case of a large, high-pressure facility, a blow-off diaphragm will be added to vent excess gas; otherwise, the volume of the receiver tank might be excessive.

The test section is an area that represents the greatest compromise in initial design. To assure constant stream conditions over the long test section, the cross-sectional area must increase to compensate for the boundary-layer growth. Unfortunately, the boundary-layer growth is dependent upon the pressure and enthalpy levels of the airstream. Therefore, the divergence rate of the walls must be set for a special range of tunnel running conditions. Airstreams generated by conditions off these design points will result in either an expanding or contracting airstream, which results in complications in reducing the aerodynamic data (see Chapter 7, Section 10.2). The wider the range of stream conditions designed for, the more nonuniform will be the off-design airstreams. In order to maintain airstream uniformity, the range of conditions must be limited or else adjustable walls provided. Wall adjustment, however, is incompatible with the requirement for good vacuum sealing.

5.3.1.1 Gas Compression Cycle

To illustrate the operation of the drive system, the sketches in Figure 5.14 show schematically the time history of the gas cycle. The description is intended only to define the various phases of the gas-compression cycle, which follows bursting of the main diaphragm.

5.3.1.2 Tailoring Requirement

To utilize a shock-tube-drive system in a counterflow facility, the stagnation region, or reservoir, must remain at constant pressure for a long enough time to complete the model flight. A constant reservoir condition can be accomplished by operating the shock-tube in a "tailored" condition. This means that the returning shock wave that brings the air and driver gas to zero velocity also leaves these two gases at the same pressure. With no pressure differential across the air/driver-gas interface, the reservoir will remain at nearly constant pressure until the expansion wave arrives to end the cycle. Testing time is then dependent upon the arrival of this expansion wave, a fact which leads to designs favoring long driver tubes.

Operating the shock-tube in a "tailored" mode limits the operation to a unique set of stagnation enthalpy conditions. The "tailoring" requirement

$$\frac{\gamma_u}{\gamma_1}\left(\frac{p_2}{p_1}\right)\left(1 - \frac{(p_2/p_1) - 1}{\gamma_1 M_s^2}\right) = \left(\frac{a_u}{a_1}\right)^2 \left(1 - \frac{\gamma_u - 1}{a_u/a_1}\,\frac{M_s}{2}\,\frac{(p_2/p_1) - 1}{\gamma_1 M_s^2}\right)^2 , \tag{5.4}$$

where γ = ratio of specific heats, C_p/C_v

p = pressure, newtons/m^2

M_s = shockwave Mach number

a = speed of sound, m/sec

subscripts

1 = initial loading conditions in shock-tube

2 = conditions behind shockwave

4 = conditions in driver tube just prior to bursting main diaphragm

essentially reduces to the fact that given the acoustical ratio (a_u/a_1) across the main diaphragm and the specific heat ratios, γ_u, and γ_1, there is only one M_s that will "tailor". While this seems like a limiting factor, in reality it merely sets the nozzle throat diameter and operating points for a given driver gas in the facility.

The counterflow facility that is shock-tube-driven may be constructed with a single nozzle contoured for a specific Mach number and still allow the free-stream velocity to be varied by changing the reservoir enthalpy. This makes it unnecessary to change the complete nozzle to change test-section air velocity. Only the throat diameter need be changed, and this can be done by changing a throat insert. The required relation between reservoir enthalpy and throat area ratio is shown in Figure 5.15 (Ref.5.19). The throat blocks are machined to match the specific reservoir conditions dictated by the "tailoring" requirements and the driver-gas conditions available.

5.3.1.3 Shock-Tube-Drive Capabilities

The shock-tube-drive system is able to develop high-energy reservoirs, and consequently, high-velocity airstreams. Figure 5.16 shows the relationship of shock-wave Mach number in the shock tube and airstream velocity in the test section. Indicated on this plot are typical "tailored" operating points – two for cold driver gases, and two for commonly used combustion-heated-helium drives. Thus, it is apparent that not only can a high-stream velocity be established by a shock-tube-drive system, but that the stream velocity can be varied over a wide range.

In a facility with the nozzle Mach number fixed, varying the airstream velocity is necessarily accompanied by changes in the speed of sound and free-stream temperature in the test section. The variable free-stream temperature, however, rather than being a disadvantage, actually permits a wide range of total Mach numbers and Reynolds numbers to be obtained.

5.3.2 Limitations of the Shock-Tube Wind Tunnel in a Counterflow Facility

The advantages of this type of test facility to extend the testing range are, unfortunately, accompanied by operating problems which put definite limits on its use. First, there is the necessity for timing the arrival of the model to match the establishment of the airstream. While at Ames Research Center, this has not been a major problem area, for some guns there could be enough uncertainty in launch time to make timing a problem.

Another major problem with the shock-tube drive is that of contamination of the airstream. When the reservoir is established and airflow is started through the nozzle, there is a tendency for the driver gas to mix with the air at the interface and flow through the nozzle before the end of the predicted clean-flow period. Small amounts of driver-gas contamination cannot be detected by pressure measurements and therefore the true air test time may not be conclusively known. The use of other techniques to determine when contaminated flow begins is therefore required.

For aerodynamic testing, small contamination is not too serious, but it can introduce serious errors into the measurements of shock-layer radiation from models, for example. In addition to chemical contamination, it is also found that because of the violent nature of diaphragm opening and high-stagnation enthalpy at the nozzle,

metal appears in the airstream in the form of small particles. Again, the amount of this type of contamination is not enough to affect most aerodynamic measurements, but may have important consequences in some tests, for example, boundary-layer transition testing if the particles hit and roughen the model surface.

Another operating problem is that of accurately determining the airstream properties. Since running time is in the millisecond range, fast-response gages are necessary. These gages have an electrical output and require calibration periodically. Unfortunately, such calibration is frequently static in nature while the use of the gage is dynamic. The method used to assure accurate results is to use redundant gages and average the results (eliminating any obviously wrong values).

Parallel with this problem of stream measurement is the additional one of stream calibration prior to testing. Pitot and static pressure measurements need to be made across the instrumented section of the facility in order to relate wall measurements to centerline values. Because of the required test-section length, stream calibration needs to be performed at many stations and at many pressure and enthalpy settings in order to determine the axial variation of the stream. This lengthwise calibration causes the stream calibration to be a long and involved procedure.

A final disadvantage of a counterflow facility is that it is much more expensive to build and requires more facility time and more man-hours per test than a conventional still air ballistic range. The cycle time per test is necessarily lengthened by the requirement to disassemble, clean, reassemble, and charge gases into the long tubes. There are also numerous expendable parts required. Typically, two preformed diaphragms and a mechanism for opening the main diaphragm are expended for each test.

5.3.3 Facility for Shock-Wave Impingement Effects on Free-Flight Models and Flow Fields

Before continuing with the counterflow facilities described above, let us examine a unique ballistic range using the shock tube driver without a nozzle. This type of facility[5.20] uses a shock-tube with a single photographic station to study the effect of shock wave impingement on models in free flight. The model is launched into the shock tube so as to be in the field of view of the window at the same time as the shock wave. Multiple photographs are made of the interaction of the normal shock wave with the model and its wake.

The critical factor in testing with this type of facility is in timing the arrival of the model and shock wave to coincide at the instrumented station. For windows of the order of 0.5 meter in length and model velocities of 5 km/sec, the time allowable for coincidence of model and shock wave at the test station is 100 μsec. This degree of timing accuracy is achieved by using a short shock tube and a long flight range, as is shown in Figure 5.17. The model is launched and its velocity is measured with a series of detectors. With this velocity information, the arrival time of the model at the window is computed. This information is fed to a delay unit which then fires the shock tube so as to produce a normal shock wave at the predicted time of arrival of the model at the window.

The photographic information obtained can be related to shock Mach number and model velocity. A very wide range of shock Mach numbers can be utilized as there is no necessity to tailor the drive conditions. The model velocity also can be varied almost at will as the only requirement is timing for one point in space and not over a protracted test-section length.

5.3.4. Hypervelocity Free-Flight Aerodynamic Facility

Of the four high-performance, short-duration, counterflow facilities which have been built at Ames Research Center[5.21], we will choose the largest for discussion and description in detail. It is called the Hypervelocity Free-Flight Aerodynamic Facility. The facility is shown in the sketch in Figure 5.18. The general structural arrangement is designed to allow approximately 0.025 sec of usable flow time in a test section 23 meters long. The test section is large enough to allow model excursions of ±20 cm and remain within the photographic field of view. Models up to 3.8 cm in diameter are possible with the largest available gun. The guns are interchangeable on a fixed, prealigned gun beam 46 meters long.

5.3.4.1 Operating Range and Boundary-Layer Correction

The airstream capabilities of this test facility are shown in Figure 5.19. These values are functions of the present operating pressure limit (680 atm) and the preselected Mach number of the airstream (M = 7).

Three interchangeable nozzle throat inserts are available to match the three different reservoir enthalpy conditions: H_s = 1870 joules/g (cold helium/air drive), H_s = 4670 joules/g (combustion-heated helium/air drive), and H_s = 7500 joules/g (another mixture of combustible gases with helium/air drive). As is noted in the figure, these reservoir conditions give airstream velocities of 1.8, 2.9, and 3.7 km/sec.

The two combustion-heated drives differ in the mixture of gases loaded, thus yielding end products of combustion having different final temperatures, molecular weight, and values of γ. As an example, for a reservoir enthalpy of 4670 joules/g, the mixture loaded is

$$4.5(H_e) + 3.5(N_2) + 1.0(O_2) + 3.0(H_2) \qquad (5.6)$$

For convenience and economy, air is used instead of N_2 and O_2.

$$4.5(H_e) + 4.43(air) + 0.07(O_2) + 3.0(H_2) \tag{5.7}$$

This combustion mix will tailor in this facility at a shock-wave Mach number of about 5.8.

The combustion-heated helium drive is used in preference to a cold hydrogen drive (which gives approximately the same stagnation enthalpy) in the interest of safety. In the combustion mode, hydrogen is used but in relatively small quantities. While some degree of hazard exists with the possibility of detonation instead of smooth burning occurring with the H_2, O_2, H_e mixes, operating results have shown consistently good burning with the driver geometry available.

The driver tube for this facility is 0.43 meter inside diameter and 23 meters long (length/diameter = 53.5). Ignition of the combustible mixture is accomplished by heating a single 0.38-mm-diameter tungsten wire with a pulse from a 90 microfarad bank of capacitors charged to 14.5 kV. Used in this manner, the wire is heated and not exploded, thus giving a line ignition down the center of the tube. The wire is installed with sufficient tension to keep the sag below 1 cm.

The pressure capability of the shock tube and driver tube is rated at 2040 atm with a safety factor of 1.5. This rating gives a good allowance for any adverse burning conditions.

Higher velocities than the 3.7 km/sec shown can be obtained by adjusting the constituents of the combustion drive. However, as is noted in the figures, the free-stream density drops rapidly with increasing stream velocity and aerodynamic testing in airstreams above 4 km/sec would be highly limited for this particular facility. Obtaining a higher free-stream density at higher airstream velocities by increasing the reservoir pressure is possible but is presently limited due to operating limits imposed by the main diaphragm (at 680 atm, this diaphragm is 1.27-cm thick, 304 stainless steel).

Another limitation on the use of a wider range of shock wave drives is that of maintaining uniform test-section conditions. As mentioned earlier, the test section must be constructed with a diverging test section to compensate for boundary-layer growth. The rate of the boundary-layer growth with distance has been calculated for this facility and is shown in Figure 5.20. These slopes are based on flat-plate turbulent boundary-layer growth at a distance of 37 meters from the leading edge.

The divergence rate built into this facility is 0.007 cm/cm, which matches the boundary-layer growth at $M_s = 10$ at 700 atm. This divergence rate was chosen as it was intended to operate the facility at high pressure at high-reservoir enthalpies. Lower pressures were contemplated for use with the lower reservoir enthalpies.

The result of operating off design is shown in Figure 5.21. To prevent the possibility of confusion with regard to this figure, it must be realized that the airflow is from station 16 to station 1, while the model flies from station 1 to station 16. This figure is so constructed so as to indicate the density experienced by the model at the time it passes through each station. This record of free-stream density shows clearly an expanding stream where the boundary-layer-growth rate is less than the wall-divergence rate. In this particular example, the stream effectively expands more than predicted by differences in boundary-layer correction. Figure 5.22 shows the stagnation-pressure record for this test. Indicated on the record are the pressures, which, when translated downstream, affected the flow at the time the model appeared in the stations. Thus, the rising reservoir pressure alone created a 18-percent change in the stream pressure that affected the model from station 1 to station 16. It is possible that a modification to the reservoir pressure history by varying the shock-tube loading so as to decrease pressure with time could be used to compensate for expansion of the airstream in the off-design operation. Success of this type of operation could greatly enhance the operating range of the facility.

5.3.4.2 General Test Range Capabilities of this Shock-Tube Facility

A general picture of the range of conditions that can be presently covered is shown in Figure 5.23. The results are based on a rather cautious maximum model velocity of 6 km/sec (compared to a maximum-recorded gun velocity of 11 km/sec) and a maximum model diameter of 3.8 cm. This choice is made to allow for the use of models with more complex shapes and greater weights than the minimum length plastic cylinders used in highest velocity firings; that is to say, it perhaps represents the usual velocity of the kinds of models of interest in aerodynamic testing. As can be seen, the velocity capability has been increased by more than 50% while still retaining a useful range of Reynolds number. The advantage of the counterflow airstream is even more pronounced when the model velocity is restricted by structural limitations to a value lower than 6 km/sec. However, because of the short running time of this facility, a minimum model velocity of approximately 2 km/sec is required if a countercurrent airstream run through the full length of the test section is desired.

5.3.4.3 Time and Coordination Problems

This imposition of a minimum model velocity is but one of the ramifications arising from the facility's short run time. To illustrate, Figure 5.24 shows a time-distance plot of the operation of this facility. This time history was taken from a test in which the airstream velocity was 2.9 km/sec and the model velocity was

3.7 km/sec. As shown on the diagram, with perfect timing, a minimum model velocity of 1.2 km/sec could be accommodated. However, to be realistic, leaving about 2 to 3 msec on both ends for timing margin, the minimum model velocity rises to the practical value of about 2 km/sec.

Expanding more on this timing problem, the example shown in Figure 5.24 was made with a relatively small gun, 1.27 cm diameter. This gun, for the velocity shown in the example, normally takes 0.042 sec between the signal to fire the gun and arrival of the model at station 1. From the time-history plot, it is seen that the gun is fired at the same time that the main diaphragm was ruptured. It is fortunate that this gun is fairly consistent in this time of model arrival as this type of coordination is the poorest possible. The greatest variation in time in the operation of these light-gas guns is in the time to burn the gun powder and set the compression piston in motion. With a larger gun requiring a longer time to place the model at station 1, the timing of the opening of the main diaphragm is determined by make-switches triggered by the pump piston after it is in motion. Smaller guns, which will have to be fired after the main diaphragm is ruptured, will have smaller errors in time because of the smaller overall time of operation.

While the timing is critical, this facility has been sized to allow a usable test time plus sufficient excess to cover expected irregularities in the operating cycle for all model velocities above the minimum 2 km/sec. Scatter in the time for the shock wave's arrival at the nozzle has been observed to be of the order of 1 msec. The gun's operation is less accurate, giving uncertainties of up to 5 msec for the worst case. These times show that, for an adverse summation of timing errors, the model can be placed outside the flow time at either the start or end of the flight.

5.3.4.4 Airstream Properties and Calibration

To accurately determine the stream parameters, four dynamic measurements are made during the gas-cycle process. These are: driver pressure at the time of diaphragm opening; velocity of the shock wave in the shock tube, reservoir pressure near the end wall of the shock tube, and test-section wall pressure. These measurements, along with previously measured air pressure in the shock tube and the loading pressure in the driver tube, give sufficient data to permit some redundancy in stream calculations.

The basic method of computing the free-stream conditions is to calculate the stagnation enthalpy from the knowledge of the shock-wave Mach number and the stagnation pressure measured (see Figure 5.25). This high-energy air is then assumed to expand isentropically to the free-stream pressure measured. This process can be traced on a Mollier diagram and yields a value for free-stream static temperature and enthalpy. The difference in enthalpy between stagnation conditions and free-stream conditions gives the value of free-stream velocity directly,

$$H_s - H_\infty = \frac{V_\infty^2}{2000}, \tag{5.8}$$

where H_s = reservoir enthalpy, joules/gram

H_∞ = free-stream enthalpy, joules/gram

V_∞ = free-stream velocity, meters/sec.

Free-stream enthalpy and temperature may be used to compute the speed of sound and stream Mach number. With this, all parameters concerning the airstream are known.

Commercially available pressure transducers (quartz crystals) are used in the driver and shock tube to measure pressure. These cells are mounted in a standard holder (standard for this facility) so that only one hole configuration is bored in the tubes. A sketch of the holder is shown in Figure 5.26. An example of the driver-pressure record is shown in Figure 5.27; the record is from a combustion-heated driver-gas test and shows the smooth burning that seems to be typical for this facility. This pressure is not used directly in any stream condition calculations, but it is necessary in determining smoothness of burning, pressure ratio across the main diaphragm, and for establishing timing relationships between ignition and rupture of diaphragm.

Two separate records are taken of the pressure in the reservoir region; the pressure transducers are placed slightly back from the diaphragm. These records are shown in Figure 5.28. The first trace shows the value of p_2, the pressure behind the shock wave as it travels towards the nozzle. The second trace shows the complete pressure history in the stagnation region. An accurate measure of p_2 from the expanded trace is useful in checking the value of shock Mach number obtained by velocity measurements.

The velocity of the shock wave is measured using piezoelectric crystals in a holder as is shown in Figure 5.29. The pressure-sensitive detectors are relatively simple to construct and rugged; some in the stagnation region have survived 50 tests over a period of two years and are still in good working order.

The final measurement required is that of free-stream pressure. The wall static pressure is measured using commercial unbonded-strain-gage cells mounted in a holder, as shown in Figure 5.30. The special holder is necessary to prevent shock and vibration of the tunnel structure from affecting the signal. The trace of a typical pressure history is shown in Figure 5.31.

With the preceding measurements, a time-distance diagram can be constructed as was shown previously in Figure 5.24. Correlating this with the time history of model position, the airstream properties can be computed for that time and position occupied by the model during its flight.

In order to define the properties of the airstream completely, measurements of stream properties across the test section at each station would be necessary. This procedure, if done for even an abbreviated set of flow conditions, would be a long and laborious task. Therefore, to date, stream calibrations have been performed only at stations 1, 8, and 15, with the flat-plate assembly shown in Figure 5.32.

The design philosophy applied to this calibration rig was to obtain as much stream information with each test as possible. Thus, the five static-pressure measurements from the flat plate, along with one wall measurement, give a fairly complete cross-stream record. This is complemented further by measurements using the two pitot probes.

Plotted in Figure 5.33 are calibration records of free-stream static pressure as a function of time from three tests at nominally the same drive conditions. To equate all measurements, the pressure is shown as the ratio of free-stream static pressure, p_∞, to stagnation pressure, p_s. As seen, the centerline pressure can differ from the sidewall pressure by as much as 20% at station 1 to almost perfect agreement at station 8.

At all stations, the central core, that is, the center 30 cm, seems to be fairly uniform. Also, station 8 seems to be not only at about the average static pressure for the entire length, but also, its sidewall pressure measurement reflects very accurately the centerline conditions.

This calibration at three distinct stations gives the end points and center of what is then assumed to be a smooth variation with distance. To check this assumption, an additional stream calibration was made by firing a sphere into the counterflow airstream and measuring its deceleration. The drag coefficients of a sphere is known and, because of a controlled small change in velocity, should be constant for the flight. By dividing the flight into segments and requiring the drag coefficient to be a preset constant value, a measurement of free-stream density can be made. The results of this method produced the tunnel density profile shown in Figure 5.21.

Along with the general determination of stream properties, some notice must be taken of possible stream contamination which, as noted earlier, could escape pressure-measurement detection. In an effort to minimize the travel of metal particles through the nozzle and into the test section, a simple modification has been made to the basic structure of the shock-tube end. This modification is primarily a baffle plate preceding the nozzle throat supported on posts. Solid metal particles traveling down the shock tube will either impact on the plate or on the end of the shock tube. No direct path is available to a heavy particle from the shock tube into the nozzle throat. The flow area available around the plate is made large with respect to the throat area so that gas velocities are low. Observations of stagnation pressures in the reservoir region and static pressures in the test section for similar tests have shown no discernible effect of the presence of this plate on the airflow. The only drawback to this plate is that it will suffer considerable damage from models, being directly in the line of sight of the gun.

Since the problem of stream contamination by the driver gas is potentially very serious, a great effort has been expended on developing means of detecting and measuring its extent. To date, the most effective, but difficult, method is that utilizing gas sampling valves and a gas chromatograph.

The gas-sampling valves are normally closed valves sealing off a previously evacuated chamber. These valves are placed in the test section within the usable core of the flow. At a preset time, the valves open for a period of 1 msec and then close, trapping a sample of gas. With multiple valves set for staggered times, a timewise sampling of the gas in the stream can be accomplished. Immediately after the test, the gas is analyzed with a gas chromatograph. The gas chromatograph can easily separate out small traces of the light gases, hydrogen and helium, from the heavier gases making up air. This gives an accurate measure of the onset of driver-gas contamination. The operating problem with this equipment is to prevent leakage into the sampling chamber before the sample is analyzed.

5.3.4.5 Operating the Facility

Because of the large size of this counterflow facility, routine operations such as separating the joints, cleaning the tubes, and installing diaphragms can become major operations. Therefore, in the design, thought was devoted to mechanizing these operations and reducing the crew size needed to perform them. Reducing the cycle time was also, of course, an objective. As a result, all connections between the driver and shock tube are made up hydraulically. Photographs of the facility (Figures 5.34 and 5.35) show the hydraulic system and the methods of connection used on this structure. Only one bolt needs to be tightened to assemble the facility-that located at the nozzle joint.

Cleaning the tubes is achieved by first separating the tubes, then translating the shock tube laterally using hydraulic rams. Then a cleaning patch over a diameter-size plug is drawn through the tubes using a capstan drive. Two men can assemble this facility in about one-half hour, and disassemble and clean it in about one hour. Without the time and manpower-saving function of the hydraulic system, testing would be considerably slower and would require larger crews.

REFERENCES

5.1 Pope, Alan — *Wind Tunnel Testing.* John Wiley & Sons, 1954.

5.2 Seiff, Alvin — *A Free-Flight Wind Tunnel for Aerodynamic Testing at Hypersonic Speeds.* NACA TR 1222, 1955.

5.3 Eggers, A.J.Jr — *A Method for Simulating the Atmospheric Entry of Long-Range Ballistic Missiles.* NACA TR 1378, 1958.

5.4 Hamaker, Frank M. — *The Ames Entry Simulator and Its Application to the Determination of Ablative Properties of Materials for Ballistic Missiles.* NASA TM X-394, 1960.

5.5 Nagamatsu, H.J.; Geiger, R.E.; Sheer, R.E. Jr — *Hypersonic Shock Tunnel.* General Electric Res. Lab. Report 59-RL-2164. January 1959.

5.6 Glass, I.I, Patterson, G.N. — *A Theoretical and Experimental Study of Shock-Tube Flow.* J.Aeron. Sci., Vol.22, No.2, 1955, pp.73-100.

5.7 Whittliff, C.E.; Wilson, M.R.; Hertzberg, A. — *The Tailored-Interface Hypersonic Shock Tunnel.* Cornell Aeron. Lab. Report AD-1052-A-8, 1958.

5.8 Russo, A.L.; Hertzberg, A. — *Modifications of the Basic Shock Tube to Improve its Performance.* Cornell Aeron. Lab. Report AD-1052-A-7, August 1958.

5.9 Hertzberg, A.; Smith, W.E.; Glick, H.S.; Squire, W. — *Modifications of the Shock-Tube for Generations of Hypersonic Flow.* Cornell Aeron. Lab. Report AD-789-A-2, March 1955.

5.10 Hertzberg, A. — *The Shock Tunnel and its Application to Hypersonic Flight.* Cornell Aeron. Lab. Report AD-1052-A-5, June 1957.

5.11 Whittliff, C.E.; Wilson, M.R. — *Shock Tube Driver Techniques and Attenuation Measurements.* Cornell Aeron. Lab. Report AD-1052-A-4, August 1957.

5.12 Squire, W.; Hertzberg, A.; Smith, W.E. — *Real Gas Effects in a Hypersonic Shock Tunnel.* Cornell Aeron. Lab. Report AD-789-A-1, March 1955.

5.13 Alpher, R.A.; White, D.R. — *Ideal Theory of Shock Tubes with Area Change near Diaphragm.* General Electric Report 57-RL-19664, January 1957.

5.14 Cox, R.N.; Winter, D.F.T. — *A Theoretical and Experimental Study of an Intermittent Hypersonic Wind Tunnel Using Free Piston Compression.* ARDE Report (B) 9/61.

5.15 Bray, K.N.C.; Pennelegion, L.; East, R.A. — *A Progress Report on the University of Southampton Hypersonic Gun Tunnel.* Dept. of Aeron. Res., Univ. of Southampton, ARC Tech. Report No.457, 1959.

5.16 East, R.A. — *The Performance and Operation of the University of Southampton Hypersonic Gun Tunnel.* U.S.A.A. Report No.135, August 1960.

5.17 Stalker, R.J. — *An Investigation of Free Piston Compression of Shock Tube Driver Gas.* National Res. Council of Canada, Mech. Engr. Report MT-44, May 1961.

5.18 Kamimoto, G.; Mori, T.; Kimura, T. — *An Analysis of the Piston Motion in a Hypersonic Gun Tunnel.* Dept. of Aeron. Eng., Kyoto Univ., Japan, C.P.5, January 1964.

5.19 Yoshikawa, Kenneth K.; Katzen, Elliott D. — *Charts for Airflow Properties in Equilibrium and Frozen Flows in Hypersonic Nozzles.* NASA TN D-693, April 1961.

5.20 Merritt, D.L.; Aronson, P.M. — *Free Flight Shock Interaction Studies.* U.S. Naval Ordnance Lab., January 24, 1966. AIAA Paper No. 66-57.

5.21 Seiff, Alvin — *Ames Hypervelocity Free-Flight Research.* Astronautics and Aerospace Engineering, Vol.1, No.11, December, 1963, pp.16-23.

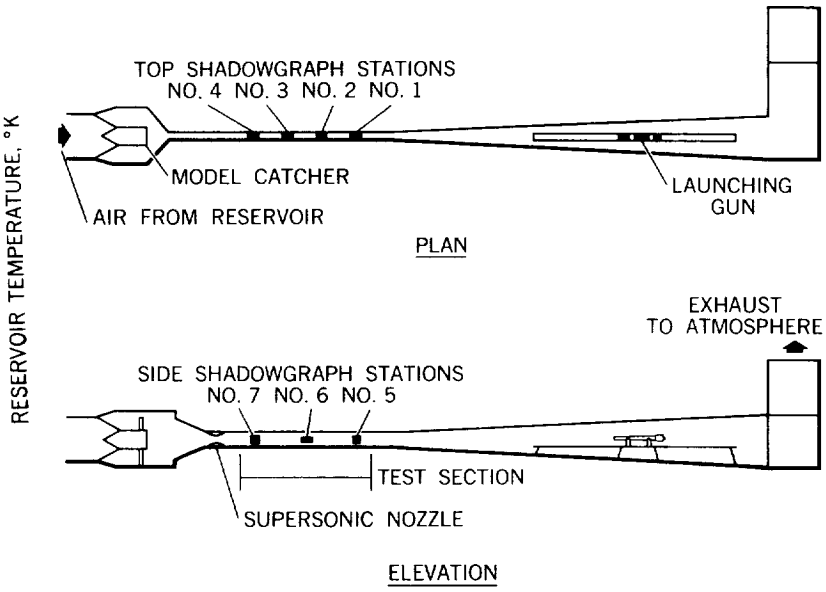

5.1 General arrangement of the Ames Supersonic Free-Flight Wind Tunnel

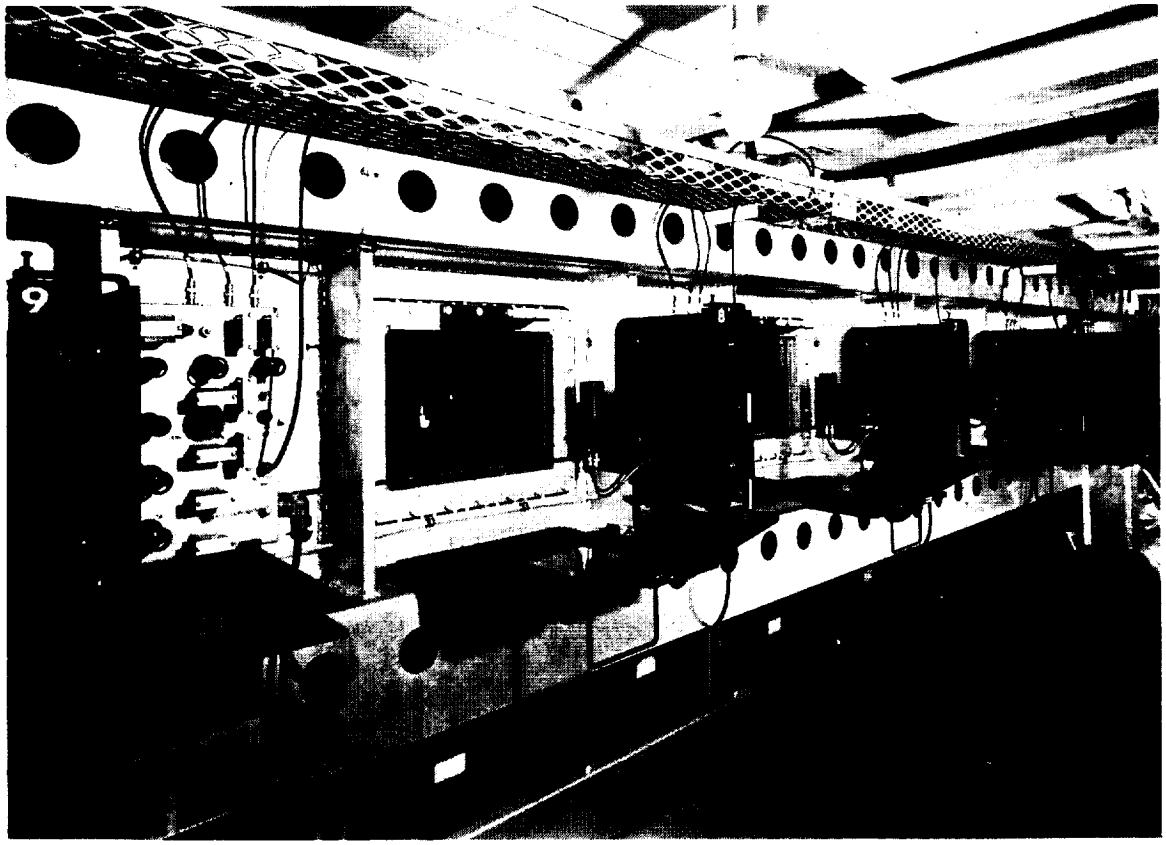

5.2 Photograph of the test section of the modified Ames Supersonic Free-Flight Wind Tunnel

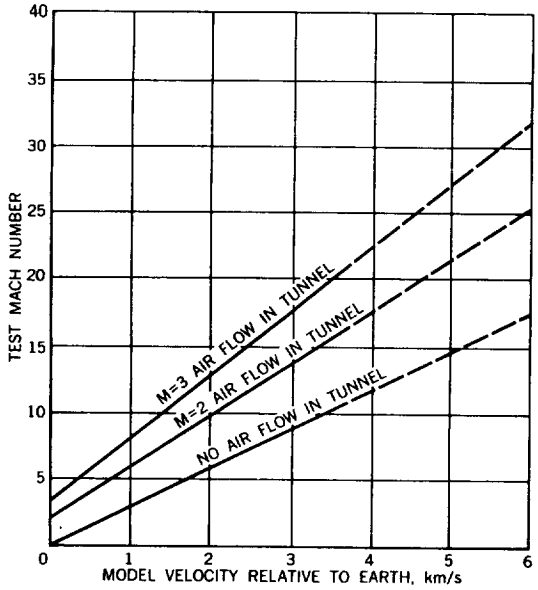

5.3 Test Mach-number capability of the Ames Supersonic Free-Flight Wind Tunnel for model velocities to 6 km/sec

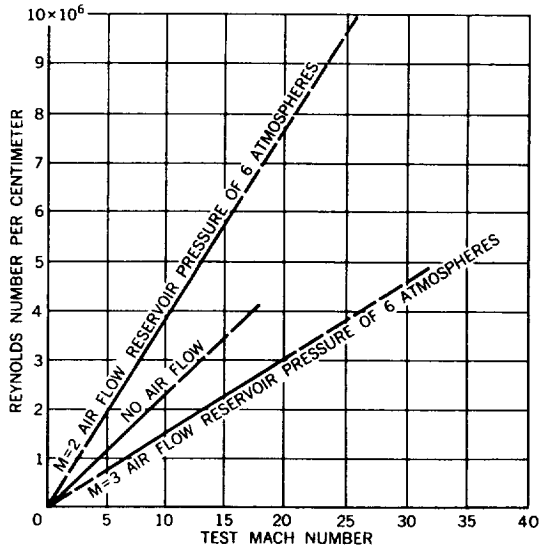

5.4 Reynolds-number capability of the Ames Supersonic Free-Flight Wind Tunnel for model velocities to 6 km/sec

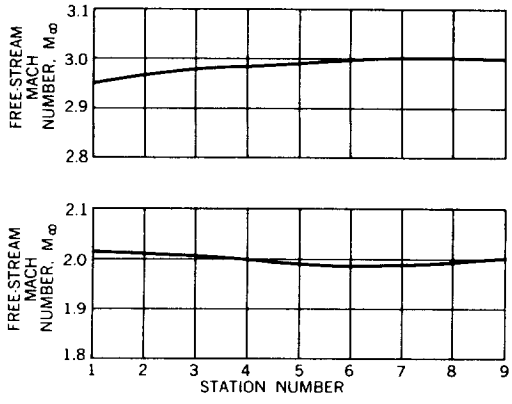

5.5 Variation of Mach number along the tunnel-centerline axis for nominal Mach numbers of 2 and 3

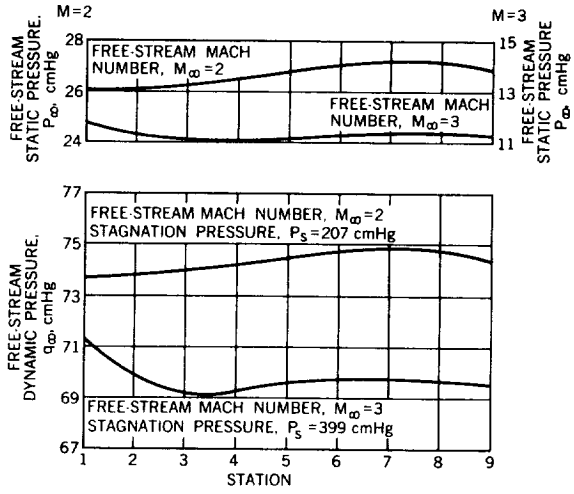

5.6 Variation of p_∞ and q_∞ along the tunnel-centerline axis for nominal Mach numbers of 2 and 3

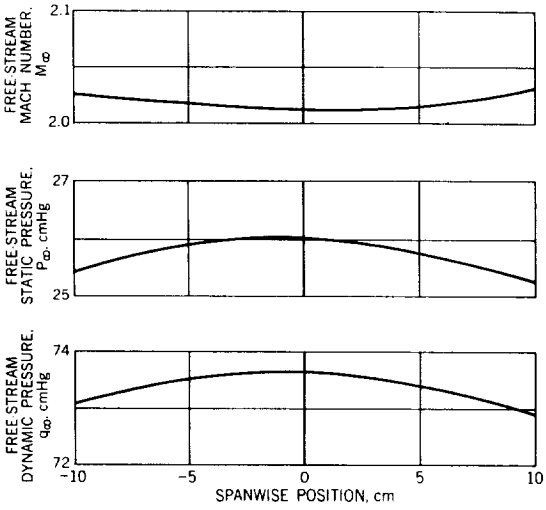

5.7 Variation of M_∞, p_∞, and q_∞ across the tunnel test section, at station 1 and on the centerline in the vertical direction, for nominal conditions of M = 2 and $p_{stag.}$ = 207 cm Hg.

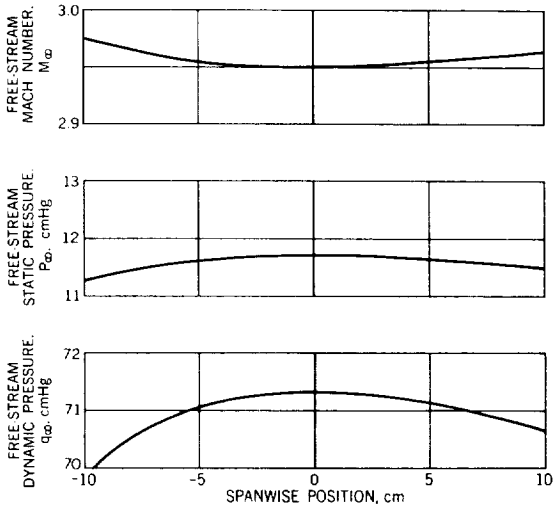

5.8 Variation of M_∞, p_∞, and q_∞ across the tunnel test section, at station 1, and on the centerline in the vertical direction, for nominal conditions of M = 3 and $p_{stag.}$ = 400 cm Hg.

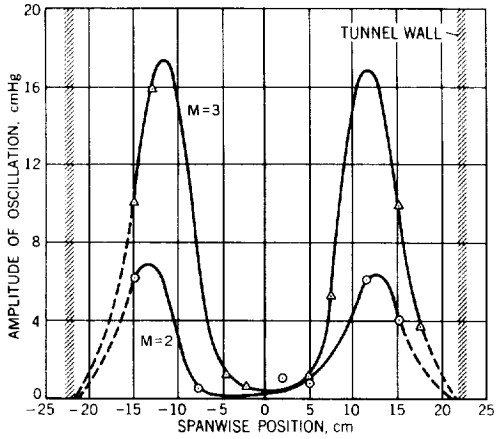

5.9 Amplitude of oscillation of the mercury manometer column used to measure the total-head pressure across centerline of tunnel at station 1, M = 2, M = 3

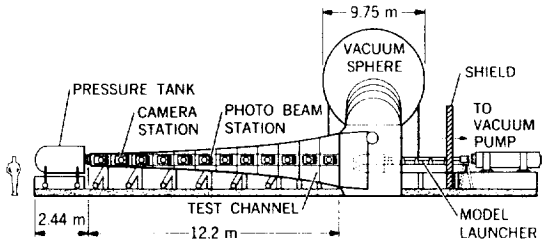

5.10 Schematic diagram of the Ames Atmosphere Entry Simulator

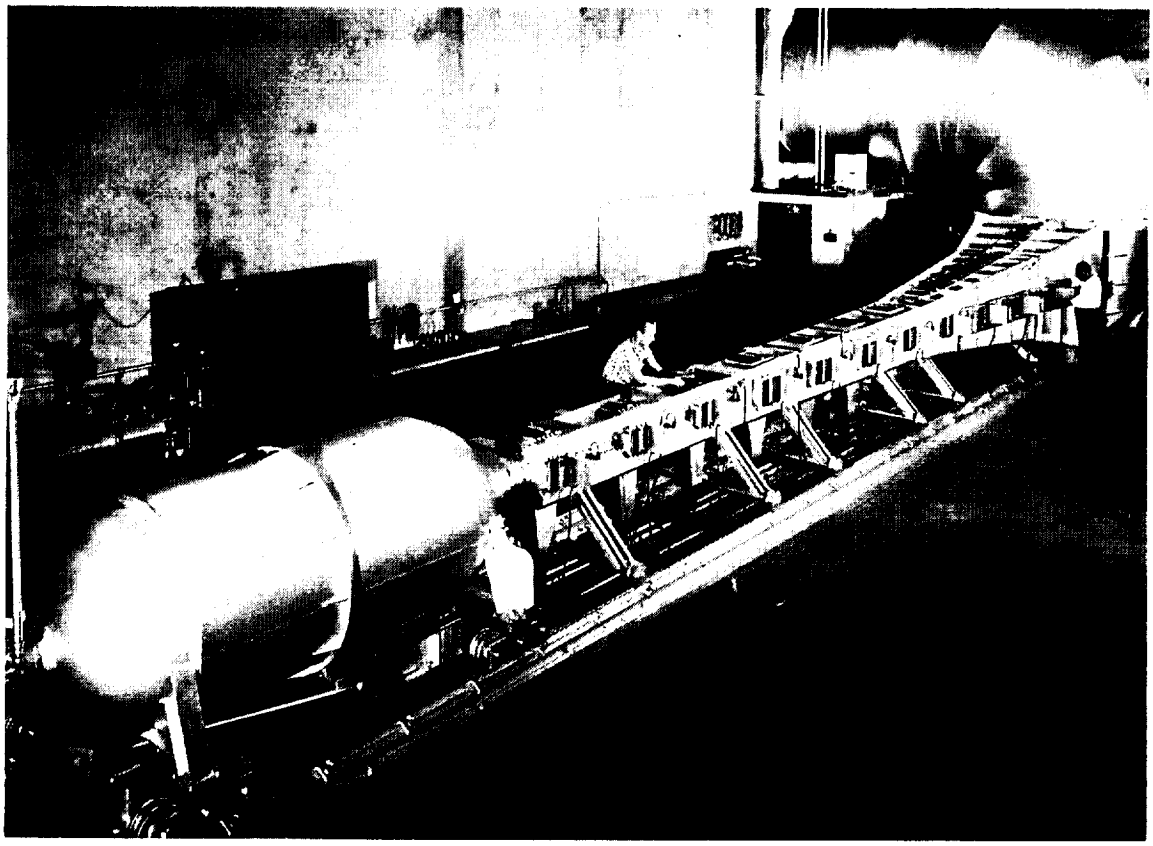

5.11 The Ames Atmosphere Entry Simulator

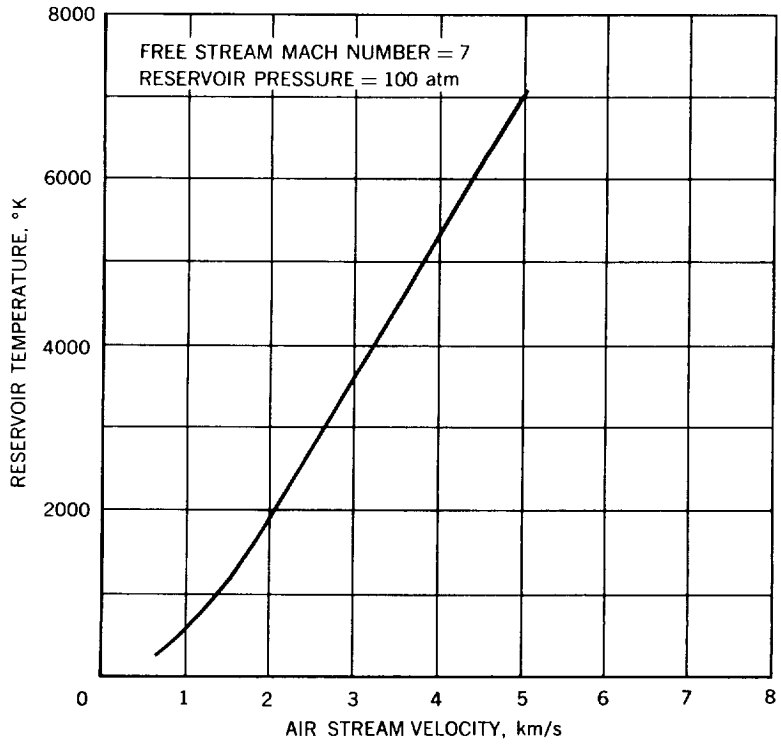

5.12 Air-stream velocity versus reservoir temperature

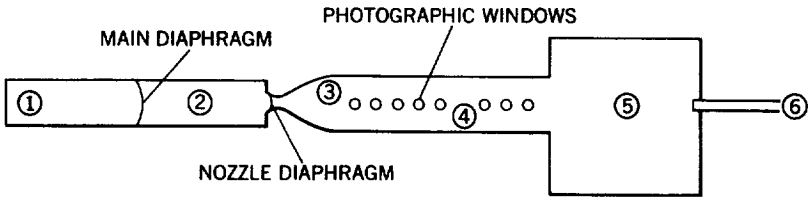

① DRIVER SECTION-HIGH PRESSURE GAS

② SHOCK-TUBE SECTION-LOW PRESSURE TEST GAS (AIR)

③ NOZZLE

④ TEST SECTION

⑤ RECEIVER TANK — SUFFICIENT VOLUME TO CONTAIN THE DRIVER AND TEST GAS AT SPECIFIED PRESSURE.

⑥ LAUNCH GUN

5.13 Shock-tube-driven counterflow ballistic facility

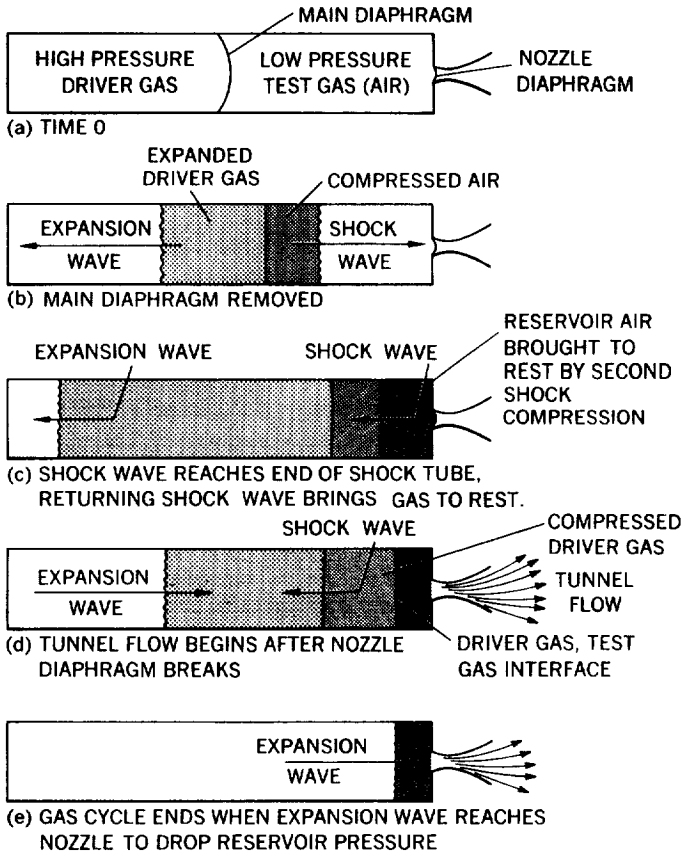

5.14 Shock-tube drive gas-compression cycle

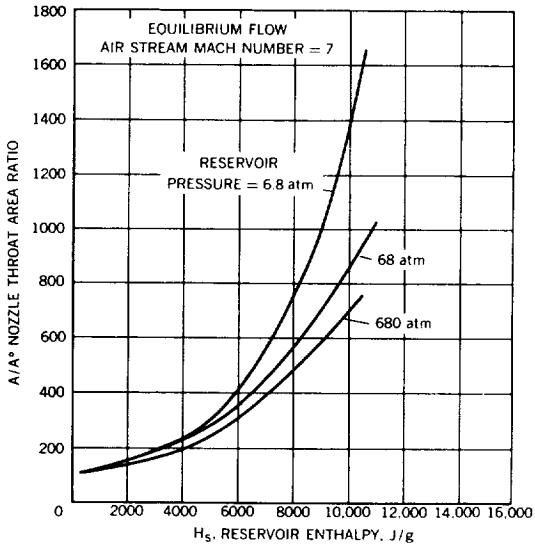

5.15 Nozzle-throat area-ratio variation with reservoir enthalpy

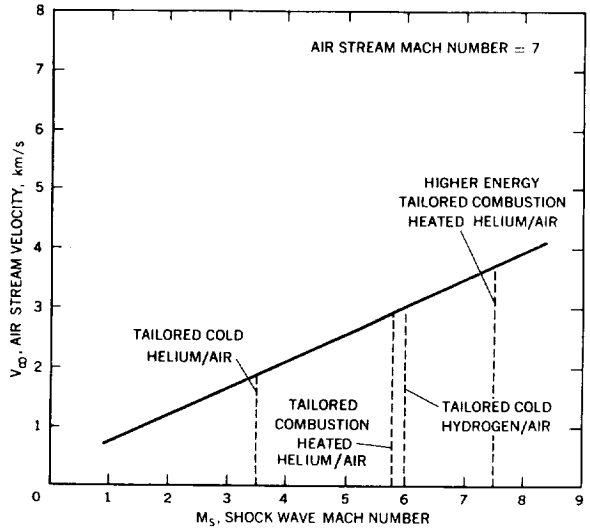

5.16 Air-stream velocity versus shock-wave Mach number

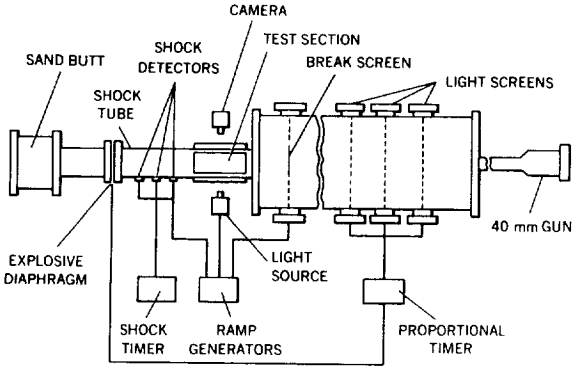

5.17 Ballistics range shock-interaction facility. (Courtesy of David L. Merritt and Phillip M. Aronson, free flight shock interaction studies, AIAA paper no. 66-57, New York, January 24-26, 1966)

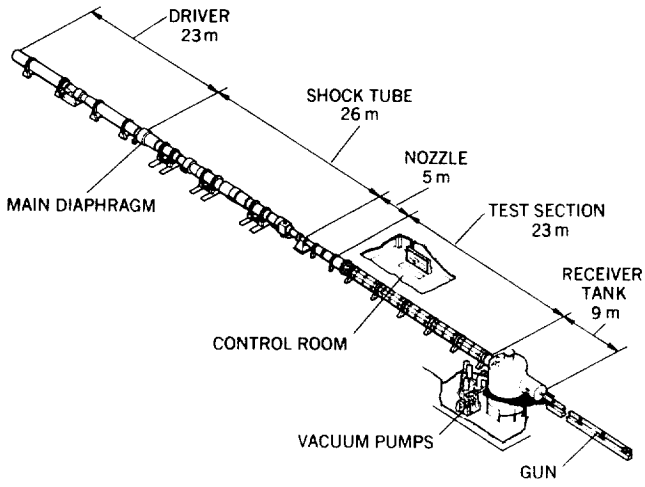

5.18 Ames Hypervelocity Free-Flight Aerodynamic Facility

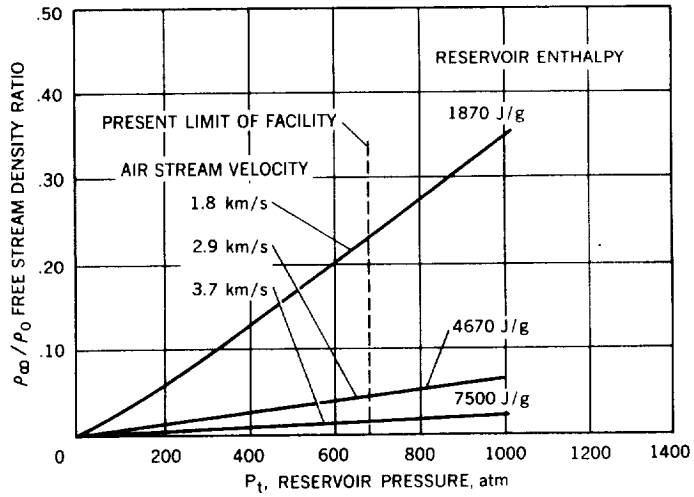

(a) FREE STREAM DENSITY CAPABILITIES

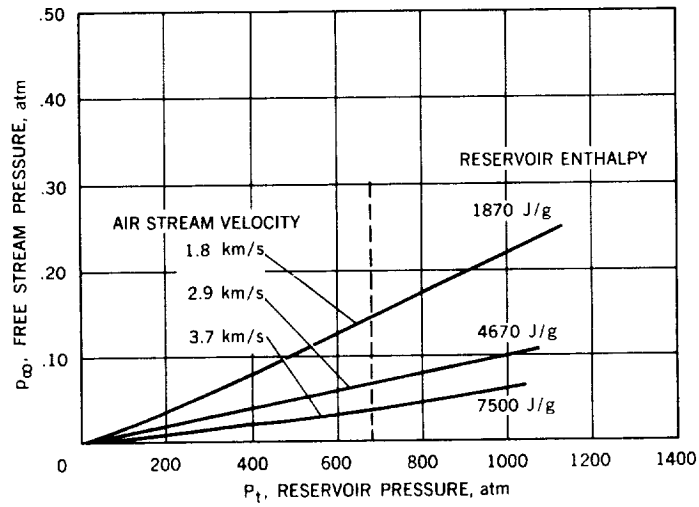

(b) FREE STREAM PRESSURE CAPABILITIES

5.19 Test-section capabilities of Ames HFF Aerodynamic Facility

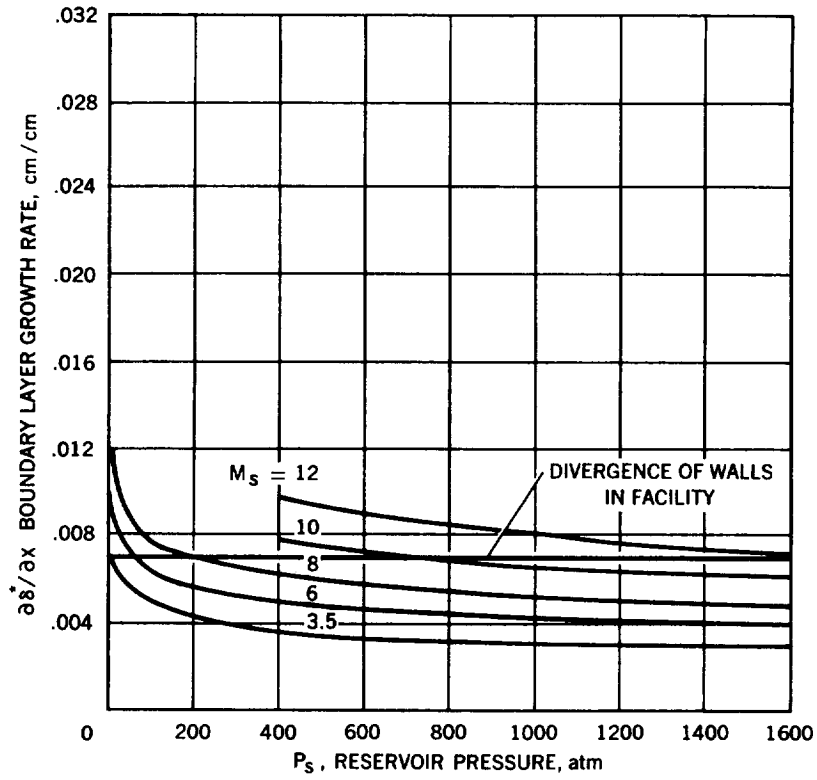

5.20 Boundary-layer growth rate calculated for Ames HFF Aerodynamic Facility

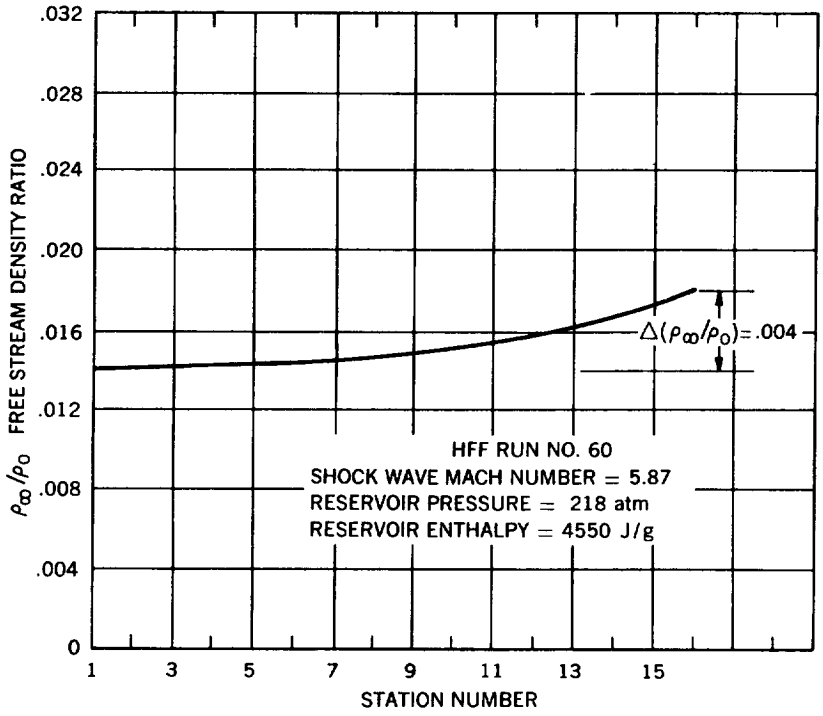

5.21 Density variation in Ames HFF Aerodynamic Facility

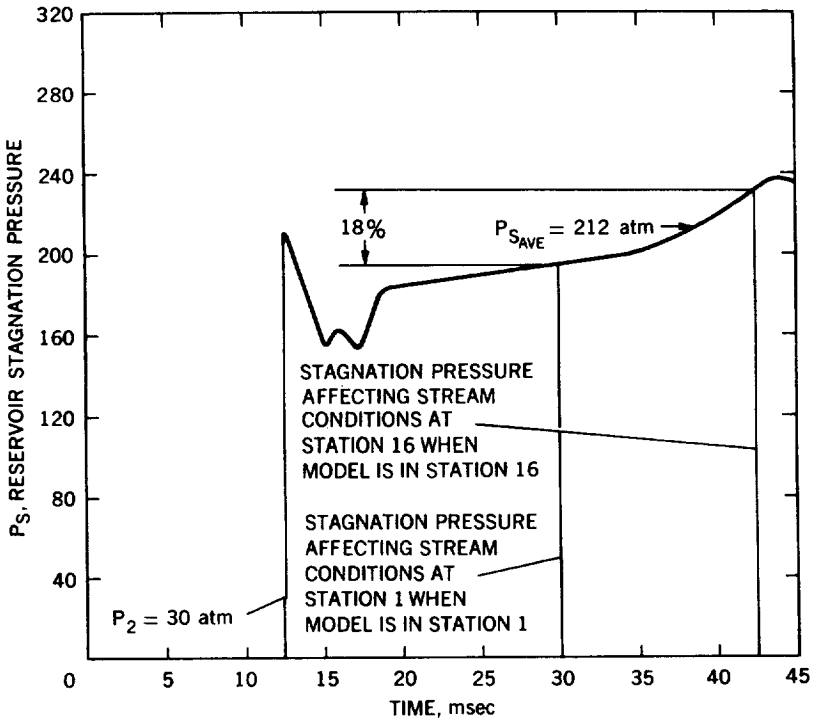

5.22 Stagnation-pressure time-history for HFF run 60

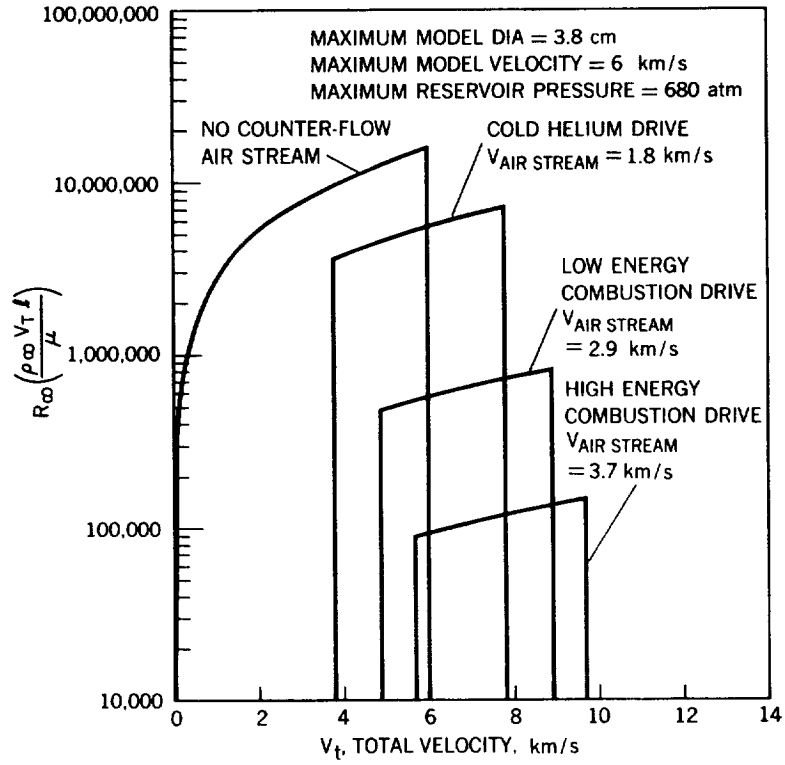

5.23 Test-range capabilities of Ames HFF Aerodynamic Facility

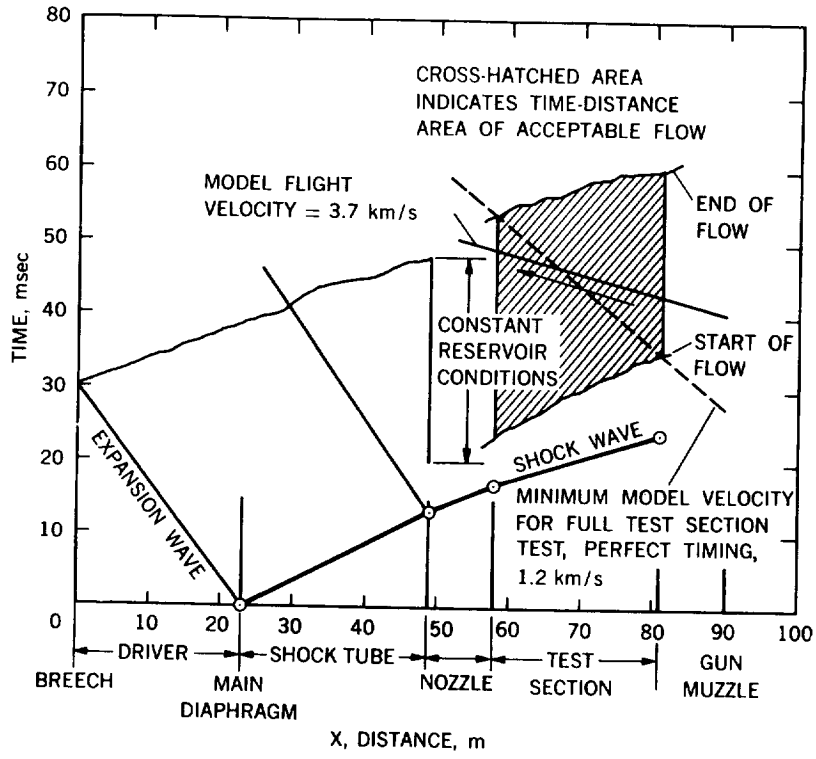

5.24 Timing relationship for Ames HFF Aerodynamic Facility

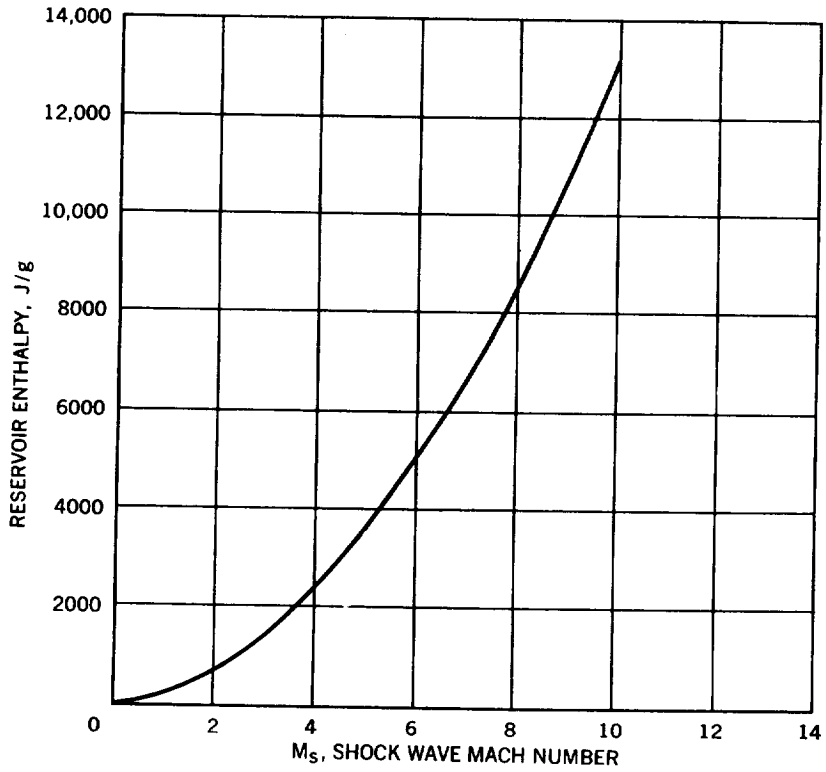

5.25 Reservoir stagnation enthalpy as a function of shock-wave Mach number

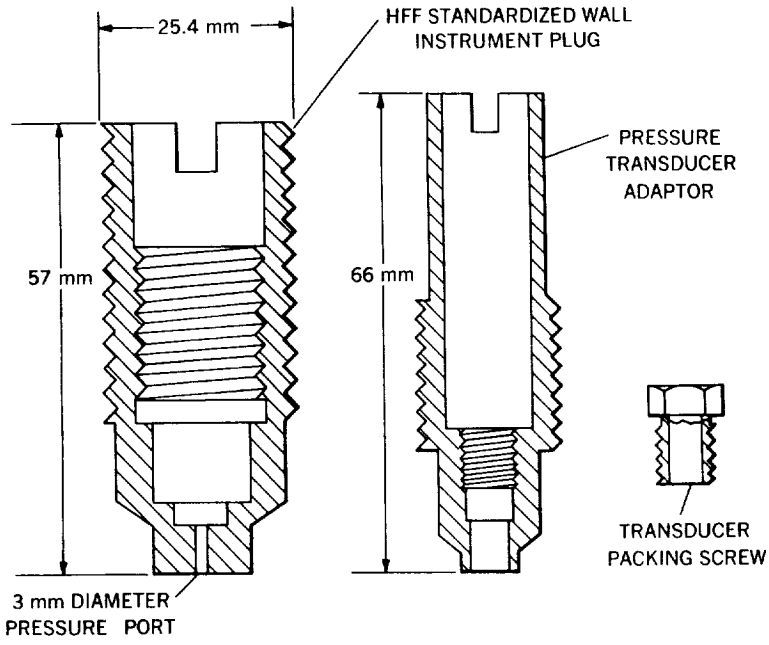

5.26 Shock-tube and driver-tube pressure-transducer holder

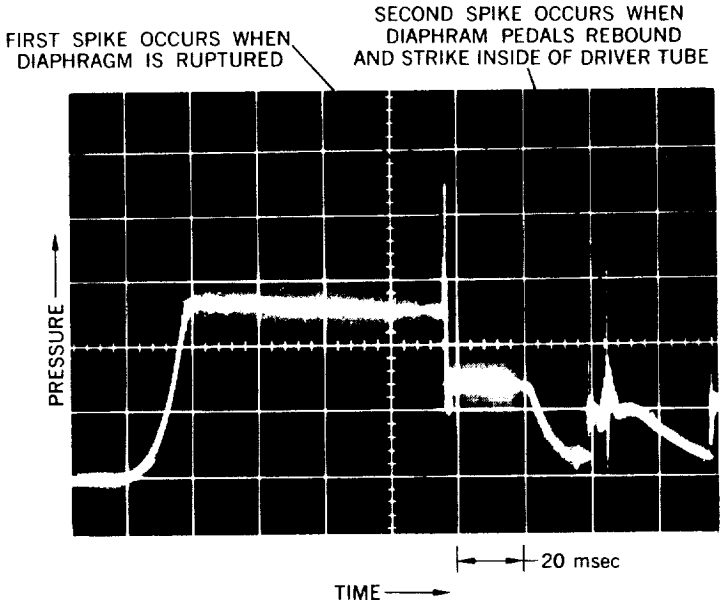

5.27 Driver-pressure time-history (combustion-heated helium)

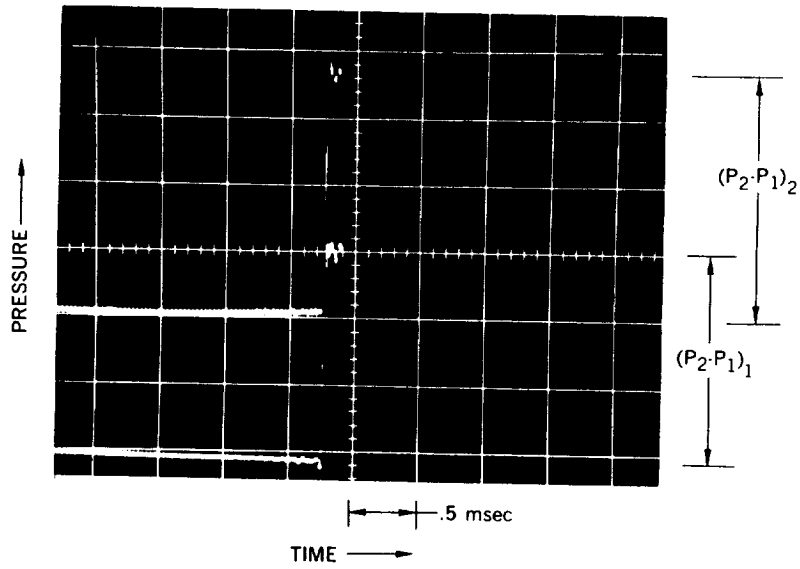

(a) EXPANDED RESERVOIR PRESSURE TIME HISTORY

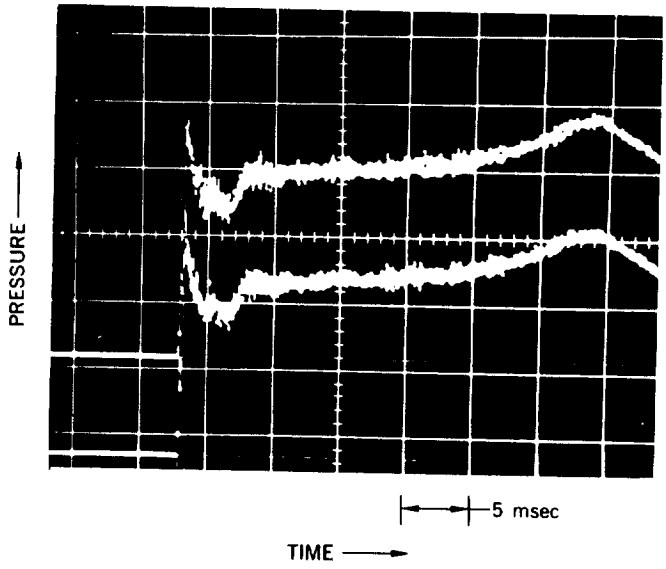

(b) REGULAR RESERVOIR PRESSURE TIME HISTORY

5.28 Reservoir-pressure time-history

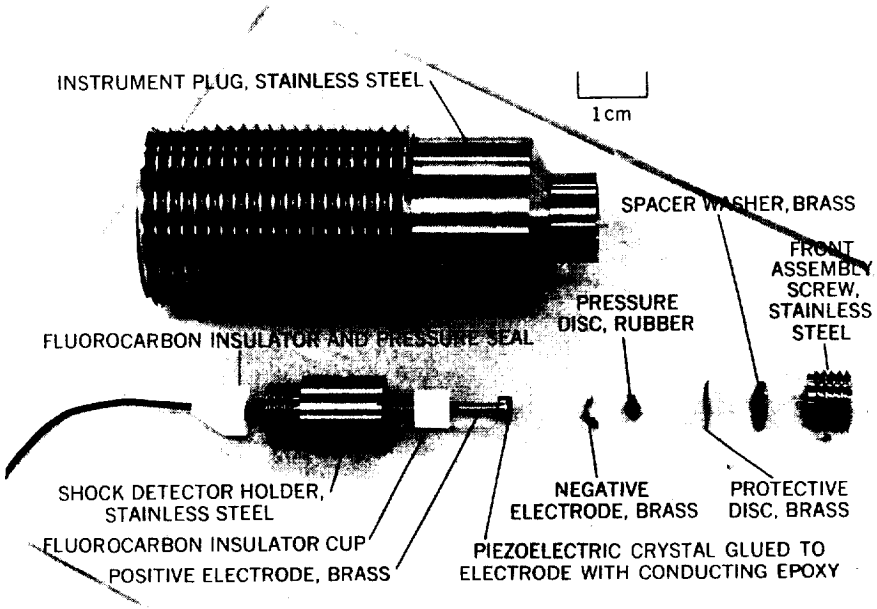

5.29 Photograph of piezoelectric-shock-detector components and holder

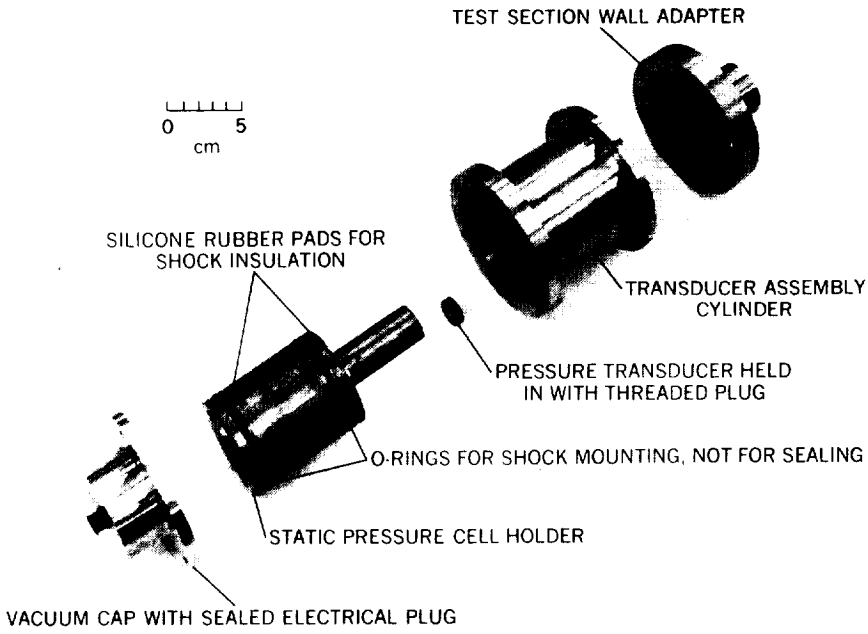

5.30 Photograph of static-pressure-transducer holder

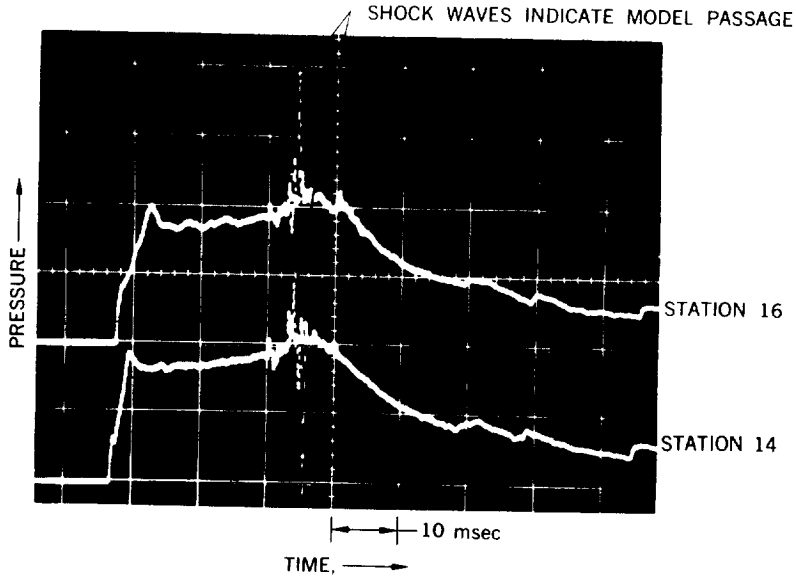

5.31 Air-stream static-pressure records

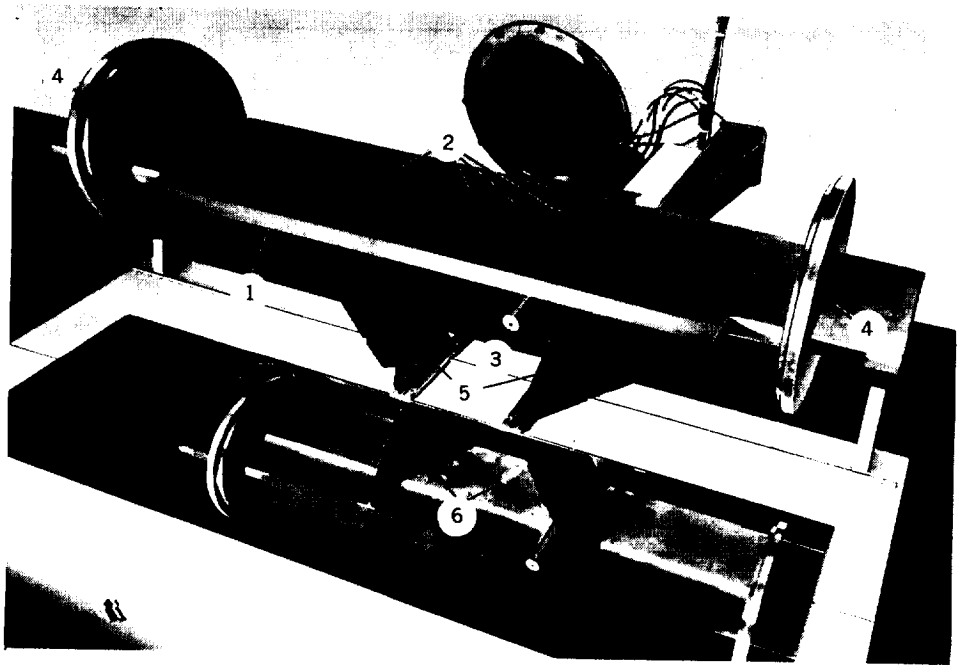

1. REPLACEABLE LEADING EDGE
2. 5 STATIC PRESSURE CELLS ON 7.6 cm SPACING
3. ONE OF TWO PITOT PRESSURE CELL HOLDERS
4. WINDOW PLATES WITH SLIDING VACUUM SEALS FOR END SUPPORT
5. CENTER SUPPORTS FOR RIGIDITY
6. PROVISION FOR OTHER PITOT PRESSURE CELL HOLDER AND ALTERNATE STING

5.32 Photograph of air-stream-calibration flat plate

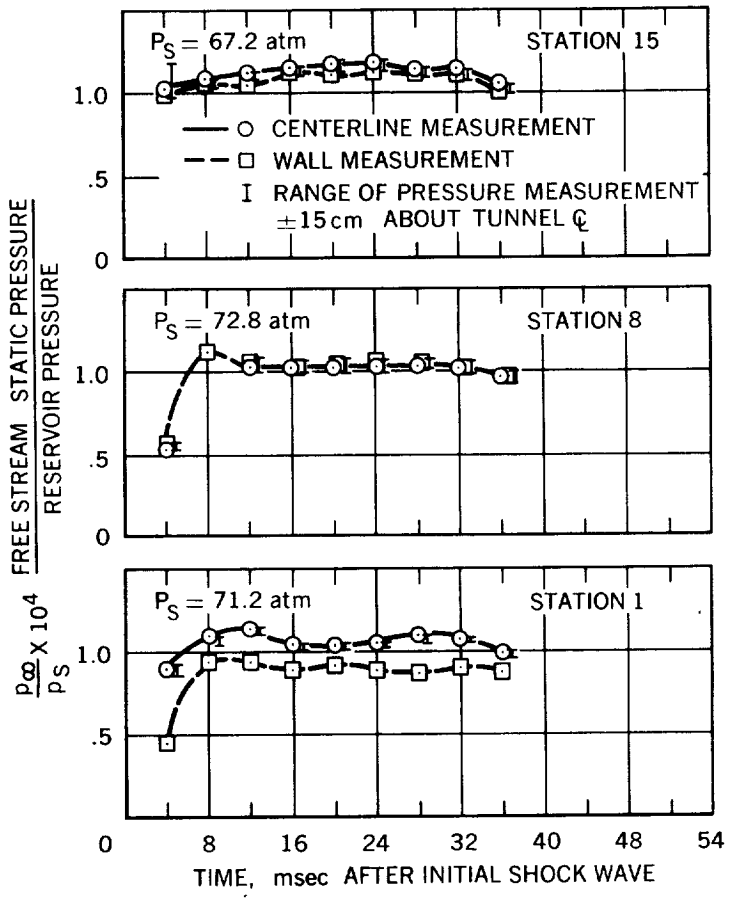

5.33 Air-stream-calibration records for three stations

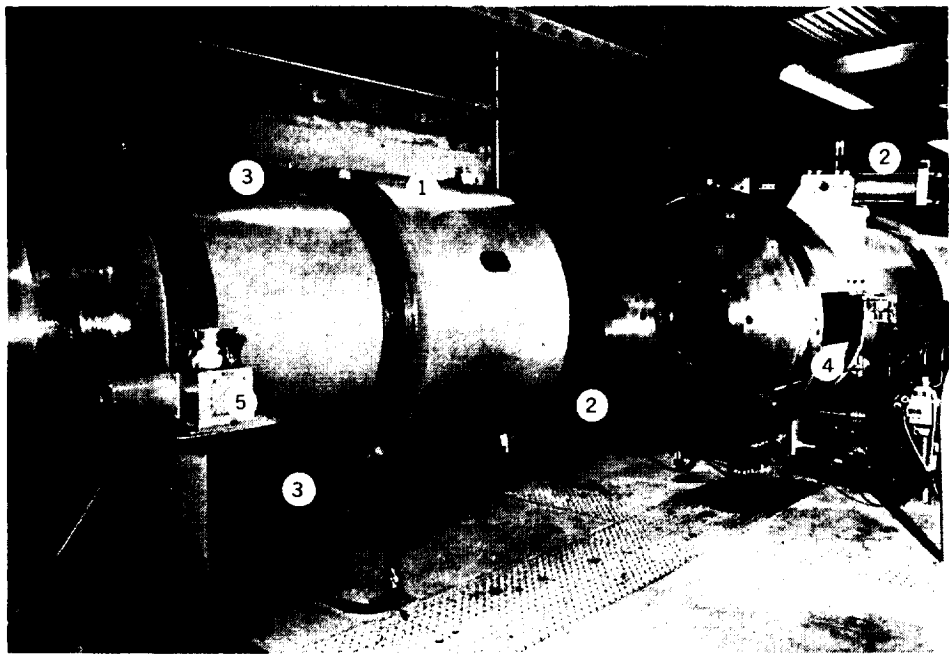

1 SHOCK TUBE, DRIVER-TUBE COUPLING NUT
2 HYDRAULIC RAMS FOR ROTATING COUPLING NUT
3 HYDRAULIC RAMS FOR TRANSLATING COUPLING NUT
4 INTERRUPTED THREADS ON DRIVER TUBE
5 CAPSTAN DRIVE UNIT FOR PULLING CLEANING PATCHES THROUGH TUBES

5.34 Photograph of Ames HFF Aerodynamic Facility, main diaphragm section

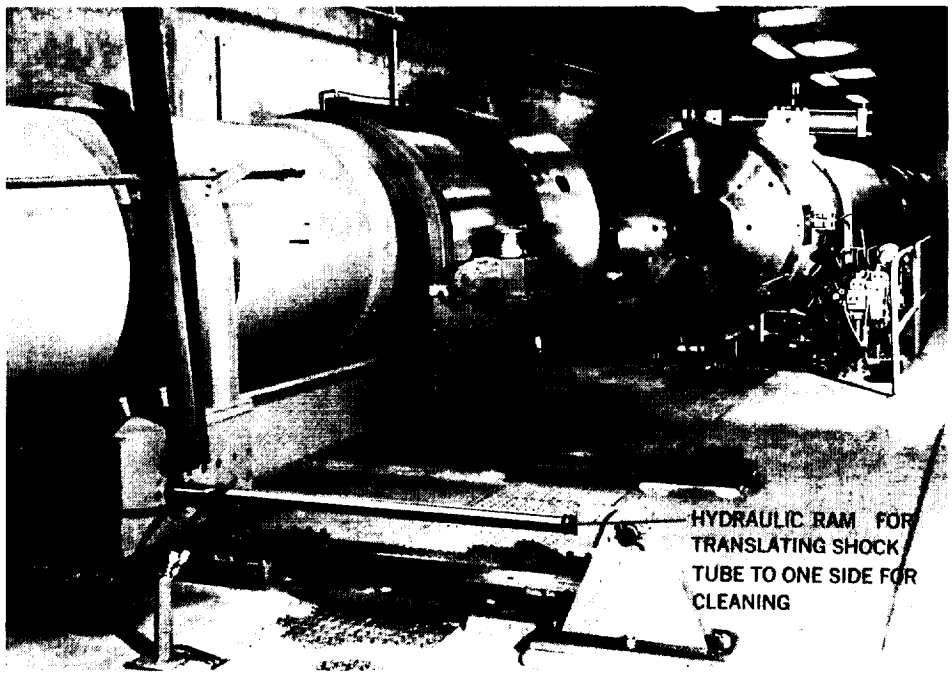

5.35 Photograph of Ames HFF Aerodynamic Facility, shock-tube-transfer hydraulic system.